

Out-of-equilibrium Anderson model at high and low bias voltages

Akira OGURI

Department of Material Science, Osaka City University, Sumiyoshi-ku, Osaka 558-8585, Japan

(Received May 22, 2002)

We study the high- and low-voltage properties of the out-of-equilibrium Anderson model for quantum dots, using a functional method in the Keldysh formalism. The Green's function at the impurity site can be regarded as a functional of a nonequilibrium distribution function $f_{\text{eff}}(\omega)$. The dependence of the Green's function on the bias voltage V and temperature T arises through $f_{\text{eff}}(\omega)$. From this behavior as a functional, it is shown that the nonequilibrium Green's function at $eV \rightarrow \infty$ is identical to the equilibrium one at $T \rightarrow \infty$. This correspondence holds when the couplings of the dot and two leads, at the left and right, are equal. In the opposite limit, for small eV , the low-energy behavior of the Green's function can be described by the local Fermi-liquid theory up to terms of order $(eV)^2$. These results imply that the correlation effects due to the Coulomb interaction U can be treated adiabatically in the two limits, at high and low bias voltages.

KEYWORDS: Kondo effect, Anderson model, Quantum dot, Nonequilibrium, Keldysh formalism

1. Introduction

The Kondo effect in quantum dots is a very active field of current research, and recent experiments¹⁻⁴⁾ have been shown to be in qualitative agreements with early predictions.⁵⁻⁷⁾ Theoretically, the equilibrium and linear-response properties of the Kondo system realized in the quantum dots have been well understood through those of magnetic alloys⁸⁾ and precise calculations with the numerical renormalization group method.⁹⁾ However, the nonequilibrium properties under a finite bias voltage V have not yet been fully understood. It is a novel problem of the strongly correlated electron systems, and has been studied extensively.¹⁰⁻¹⁴⁾

At small voltages $eV \ll T_K$ near the linear-response regime, nonequilibrium properties at low energies, i.e., at $T \ll T_K$ and $\omega \ll T_K$, can be described by the local Fermi-liquid theory,^{15,16)} where T_K is the Kondo temperature. Specifically, the nonlinear-response of the current through the quantum dots has been calculated up to terms of order V^3 based on the Kondo model¹³⁾ and Anderson model.¹⁴⁾ The coefficients can be expressed in terms of the correlation functions defined with respect to the equilibrium ground state,¹⁴⁾ and in the electron-hole symmetric case the coefficients are determined by T_K and the Wilson ratio R . In this paper, we suggest a procedure to estimate T_K and R experimentally from the differential conductance near the unitarity limit.

The main purpose of this paper is to describe a relation between the effects of the bias voltage and temperature based on a property of the generating functional Z_J for the Keldysh Green's function of the Anderson impurity. We show that Z_J can be regarded as a functional of a nonequilibrium distribution function $f_{\text{eff}}(\omega)$, and the dependence of Z_J on eV and T arises through $f_{\text{eff}}(\omega)$. From this feature of the generating functional, it is deduced that the nonequilibrium Green's function at $eV \rightarrow \infty$ is identical to the equilibrium one at $T \rightarrow \infty$. This correspondence holds exactly when the couplings between the dot and two leads are equal. Furthermore, the low-voltage Fermi-liquid behavior mentioned above

can also be deduced from this property of Z_J . As the functional of Luttinger and Ward¹⁷⁾ has played an important role in the usual Fermi-liquid theory, some of the nonequilibrium properties can be deduced from those of the generating functional.

Our results obtained in the two opposite limits of eV imply that the Coulomb interaction U can be treated adiabatically at both low ($eV \ll T_K$) and high ($U \ll eV$) bias voltages. Therefore, as one of the possibilities, we could expect that the perturbation theory in U works for all values of eV , although another possibility that a different phase of non-perturbative nature exists at intermediate values of eV could not be ruled out.

2. Keldysh Formalism for Anderson Model

2.1 Green's functions

We start with the single Anderson impurity connected to two reservoirs at the left (L) and right (R):

$$H = H_1 + H_2, \quad (1)$$

$$H_1 = \sum_{\lambda=L,R} \sum_{k\sigma} \epsilon_{k\lambda} c_{k\lambda\sigma}^\dagger c_{k\lambda\sigma} + \sum_{\sigma} E_d n_{d\sigma}, \quad (2)$$

$$H_2 = \sum_{\lambda=L,R} \sum_{\sigma} v_{\lambda} \left(d_{\sigma}^\dagger c_{\lambda\sigma} + c_{\lambda\sigma}^\dagger d_{\sigma} \right) + U n_{d\uparrow} n_{d\downarrow}, \quad (3)$$

where d_{σ} annihilates an electron with spin σ at the dot, and $n_{d\sigma} = d_{\sigma}^\dagger d_{\sigma}$. In the leads λ ($= L, R$), the excitations are described by $\epsilon_{k\lambda} = \epsilon_k + eV_{\lambda}$ and corresponding eigenfunction $\phi_{k\lambda}(r)$. To specify the static potentials V_{λ} , we introduce additional parameters α_{λ} as $V_L = \alpha_L V$ and $V_R = -\alpha_R V$ with $\alpha_L + \alpha_R = 1$. Here, the Fermi level at equilibrium is taken to be the origin of the energy. The onsite potential E_d is assumed to be a constant which does not depend of the bias voltage. The mixing matrix elements v_{λ} describe the couplings between the dot and leads, and $c_{\lambda\sigma} = \sum_k c_{k\lambda\sigma} \phi_{k\lambda}(r_{\lambda})$ annihilates an electron at the interface r_{λ} . We assume the local density of states $\rho_{\lambda}(\omega) = \sum_k |\phi_{k\lambda}(r_{\lambda})|^2 \delta(\omega - \epsilon_{k\lambda})$ to be a constant and its band width D to be infinity. We will use units $\hbar = 1$.

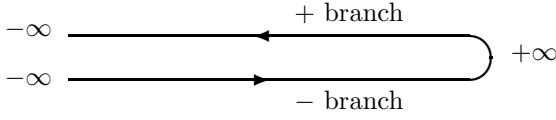


Fig. 1. The Keldysh contour of the time evolution.

In order to describe a nonequilibrium steady state realized under the applied bias voltage, we employ the Keldysh formalism.¹⁸⁾ We define four types of local Green's functions at the impurity site;

$$G^{--}(t) = -i \langle T d_\sigma(t) d_\sigma^\dagger(0) \rangle, \quad (4)$$

$$G^{-+}(t) = i \langle d_\sigma^\dagger(0) d_\sigma(t) \rangle, \quad (5)$$

$$G^{+-}(t) = -i \langle d_\sigma(t) d_\sigma^\dagger(0) \rangle, \quad (6)$$

$$G^{++}(t) = -i \langle \tilde{T} d_\sigma(t) d_\sigma^\dagger(0) \rangle, \quad (7)$$

where T and \tilde{T} denote the time-ordering and anti-time-ordering operations, respectively, and $d_\sigma(t)$ is a Heisenberg operator. Note that these functions are linearly dependent $G^{-+} + G^{+-} = G^{--} + G^{++}$, and the retarded and advanced Green's functions are given by $G^r = G^{--} - G^{-+}$ and $G^a = G^{--} - G^{+-}$. The average $\langle \dots \rangle$ is taken over the density matrix $\hat{\rho}(t)$ at $t = 0$. The initial condition is given at $t = -\infty$, where the two leads are separated from the dot and each part is in its own thermal equilibrium described by H_1 and the chemical potentials $\mu_\lambda = eV_\lambda$. Then H_2 , which includes the mixing v_λ and interaction U , is switched on adiabatically. The time evolution can be treated in the interaction representation (see Appendix A), where the Wick's theorem is applicable for the time-ordered correlation functions along the Keldysh contour shown in Fig. 1.

In the noninteracting case $U = 0$, the Green's functions which include all contributions of the mixing v_λ are given, as functions of the frequency ω (see Appendix B), by

$$G_0^{--}(\omega) = [1 - f_{\text{eff}}(\omega)] G_0^r(\omega) + f_{\text{eff}}(\omega) G_0^a(\omega), \quad (8)$$

$$G_0^{-+}(\omega) = -f_{\text{eff}}(\omega) [G_0^r(\omega) - G_0^a(\omega)], \quad (9)$$

$$G_0^{+-}(\omega) = [1 - f_{\text{eff}}(\omega)] [G_0^r(\omega) - G_0^a(\omega)], \quad (10)$$

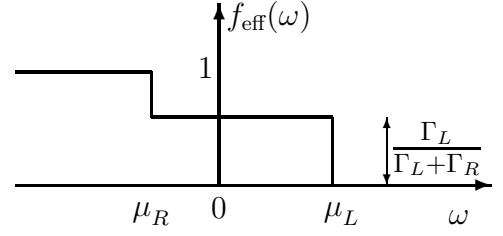
$$G_0^{++}(\omega) = -[1 - f_{\text{eff}}(\omega)] G_0^a(\omega) - f_{\text{eff}}(\omega) G_0^r(\omega). \quad (11)$$

Here $G_0^r(\omega) = [\omega - E_d + i\Delta]^{-1}$ and $G_0^a(\omega) = \{G^r(\omega)\}^*$. The level width is $\Delta = \Gamma_L + \Gamma_R$ with $\Gamma_\lambda = \pi\rho_\lambda v_\lambda^2$. The function $f_{\text{eff}}(\omega)$ expresses the nonequilibrium distribution of the electrons at the impurity site,¹¹⁾

$$f_{\text{eff}}(\omega) = \frac{f_L(\omega)\Gamma_L + f_R(\omega)\Gamma_R}{\Gamma_L + \Gamma_R}, \quad (12)$$

where $f_\lambda(\omega) = f(\omega - \mu_\lambda)$ with $f(\omega) = [e^{\omega/T} + 1]^{-1}$. At $T = 0$, $f_{\text{eff}}(\omega)$ has two steps at $\omega = \mu_L$ and μ_R as shown in Fig. 2. Note that the Keldysh formalism is applicable also in equilibrium, i.e., at $eV = 0$, where $f_{\text{eff}}(\omega)$ becomes equal to the usual Fermi function $f(\omega)$.

The Green's function for $U \neq 0$ satisfies the matrix

Fig. 2. Nonequilibrium distribution $f_{\text{eff}}(\omega)$ at $T = 0$.

Dyson equation; $\{\mathbf{G}(\omega)\}^{-1} = \{\mathbf{G}_0(\omega)\}^{-1} - \mathbf{\Sigma}(\omega)$,

$$\mathbf{G}_0 = \begin{bmatrix} G_0^{--} & G_0^{-+} \\ G_0^{+-} & G_0^{++} \end{bmatrix}, \quad \mathbf{\Sigma} = \begin{bmatrix} \Sigma^{--} & \Sigma^{-+} \\ \Sigma^{+-} & \Sigma^{++} \end{bmatrix}. \quad (13)$$

Here $\mathbf{\Sigma}(\omega)$ is the self-energy due to the interaction U . Four types of the self-energies are also linearly dependent $\Sigma^{-+} + \Sigma^{+-} = -\Sigma^{--} - \Sigma^{++}$. The perturbation theory for $\mathbf{G}(\omega)$ is described in the real-frequency (or real-time) representation, and thus the dependence of $\mathbf{G}(\omega)$ on eV and T arises only through $f_{\text{eff}}(\omega)$ which enters the noninteracting one $\mathbf{G}_0(\omega)$. This feature seen in the Keldysh formalism is quite different from that of the Matsubara formalism in which the temperature dependence arises through the summations over the imaginary frequencies.

2.2 Generating Functional

In order to see this feature of the Keldysh formalism more explicitly, we employ the generating functional Z_J that yields the perturbation of series for $\mathbf{G}(\omega)$. It is given, in the path integral form,¹⁹⁾ by

$$Z_J \equiv \int \mathcal{D}\eta^\dagger \mathcal{D}\eta e^{iS(\eta^\dagger, \eta)}, \quad (14)$$

$$S(\eta^\dagger, \eta) = S_0(\eta^\dagger, \eta) + S_{\text{ex}}(\eta^\dagger, \eta) + S_U(\eta^\dagger, \eta). \quad (15)$$

The action S consists of three parts corresponding to the free, external-source, and interaction contributions;

$$S_0(\eta^\dagger, \eta) = \sum_\sigma \int_{-\infty}^{\infty} dt dt' \eta_\sigma^\dagger(t) \mathbf{K}_0(t, t') \eta_\sigma(t'), \quad (16)$$

$$S_{\text{ex}}(\eta^\dagger, \eta) = - \sum_\sigma \int_{-\infty}^{\infty} dt \left[\eta_\sigma^\dagger(t) \mathbf{J}_\sigma(t) + \mathbf{J}_\sigma^\dagger(t) \eta_\sigma(t') \right], \quad (17)$$

$$S_U(\eta^\dagger, \eta) = -U \int_{-\infty}^{\infty} dt \left[\eta_{\uparrow-}^\dagger(t) \eta_{\uparrow-}(t) \eta_{\downarrow-}^\dagger(t) \eta_{\downarrow-}(t) - \eta_{\uparrow+}^\dagger(t) \eta_{\uparrow+}(t) \eta_{\downarrow+}^\dagger(t) \eta_{\downarrow+}(t) \right]. \quad (18)$$

Here $\eta_\sigma^\dagger(t) = (\eta_{\sigma-}^\dagger(t), \eta_{\sigma+}^\dagger(t))$ is a two component field of the Grassmann number. The label \mp specifies the branches of the Keldysh contour (see Fig. 1) where each of the components corresponds to. The Kernel \mathbf{K}_0 in eq. (16) is the inverse matrix of the noninteracting Green's function,

$$\mathbf{K}_0(\omega) \equiv \{\mathbf{G}_0(\omega)\}^{-1}, \quad (19)$$

$$\mathbf{K}_0(t, t') = \int_{-\infty}^{\infty} \frac{d\omega}{2\pi} \mathbf{K}_0(\omega) e^{-i\omega(t-t')}. \quad (20)$$

In eq. (17), $\mathbf{J}_\sigma^\dagger(t) = (J_{\sigma-}^\dagger(t), J_{\sigma+}^\dagger(t))$ is an external source of the anticommuting c -number, which is introduced for the later convenience. In eq. (18), the sign of the first and second terms are determined by that of the exponent of the time-evolution operators $\mathcal{U}(+\infty, -\infty)$ and $\mathcal{U}(-\infty, +\infty)$, respectively (see Appendix A). For $U = 0$, the path integral of the fermionic fields in eq. (14) can be evaluated analytically

$$\begin{aligned} Z_J^0 &\equiv \int \mathcal{D}\eta^\dagger \mathcal{D}\eta e^{i[S_0(\eta^\dagger, \eta) + S_{\text{ex}}(\eta^\dagger, \eta)]} \\ &= Z_{J=0}^0 \exp \left[-i \sum_\sigma \int_{-\infty}^{\infty} dt dt' \mathbf{J}_\sigma^\dagger(t) \mathbf{G}_0(t, t') \mathbf{J}_\sigma(t') \right], \end{aligned} \quad (21)$$

where $Z_{J=0}^0 \equiv \lim_{J \rightarrow 0} Z_J^0$. Then following the standard prescription,¹⁹⁾ the generating functional and full Green's function can be rewritten in the form

$$Z_J = e^{iS_U(-i\frac{\delta}{\delta J}, i\frac{\delta}{\delta J^\dagger})} Z_J^0, \quad (22)$$

$$G_\sigma^{\nu\nu'}(t, t') = -i \frac{1}{Z_J} \frac{\delta}{\delta J_{\sigma\nu}^\dagger(t)} \frac{\delta}{\delta J_{\sigma\nu'}(t')} Z_J \Bigg|_{J=0}, \quad (23)$$

where $\nu, \nu' = +, -$. In eq. (22), the fermionic fields in S_U have been replaced with the functional differentiations, $\eta_{\sigma\nu}^\dagger \Rightarrow -i\delta/\delta J_{\sigma\nu}$ and $\eta_{\sigma\nu} \Rightarrow i\delta/\delta J_{\sigma\nu}^\dagger$. The perturbation series of \mathbf{G} can be generated from eq. (23) by expanding e^{iS_U} in eq. (22) as a power series of S_U and then carrying out the functional differentiations using the explicit expression of Z_J^0 given by eq. (21). Each term of the perturbation series is written in terms of \mathbf{G}_0 and the integrations over the internal variables of real time (or real frequency). Therefore, Z_J can be regarded as a functional of $f_{\text{eff}}(\omega)$, and the dependence of $\mathbf{G}(\omega)$ on eV and T arises only through $f_{\text{eff}}(\omega)$. From this property, the behavior of $\mathbf{G}(\omega)$ at high and low bias voltages can be deduced exactly.

3. High-Voltage Behavior

3.1 General properties

We consider the behavior of $\mathbf{G}(\omega)$ in the high-voltage limit $eV \rightarrow \infty$. To be specific, we assume that the bias voltage is applied to be $\alpha_L > 0$ and $\alpha_R > 0$. In the limit of $eV \rightarrow \infty$, the chemical potentials tend to $\mu_L \rightarrow \infty$ and $\mu_R \rightarrow -\infty$, and thus the distribution function becomes a constant $f_{\text{eff}}(\omega)|_{eV \rightarrow \infty} \equiv \Gamma_L/(\Gamma_L + \Gamma_R)$, see Fig. 2. When the couplings with the two leads are equal $\Gamma_L = \Gamma_R$, the value of this constant becomes 1/2 and $f_{\text{eff}}(\omega)|_{eV \rightarrow \infty}$ coincides with the high-temperature limit of the usual Fermi function $f(\omega)|_{T \rightarrow \infty} \equiv 1/2$. Therefore, the noninteracting Green's function \mathbf{G}_0 for $eV \rightarrow \infty$ becomes identical to that for $T \rightarrow \infty$ at equilibrium. The same correspondence holds also for the full Green's function \mathbf{G} since it is determined by eqs. (21)–(23) for given \mathbf{G}_0 . Thus in the case of $\Gamma_L = \Gamma_R$ the two limits, *i*) $eV \rightarrow \infty$ and *ii*) $T \rightarrow \infty$ keeping $eV = 0$, are equivalent as far as the Green's function at the impurity site is concerned. Note that the temperature is not necessary to be kept at $T = 0$ in the $eV \rightarrow \infty$ limit. In

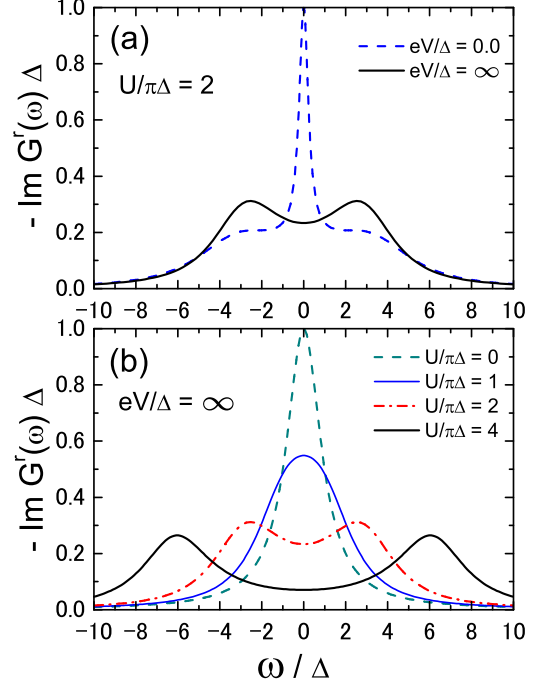


Fig. 3. Spectral function obtained with order U^2 self-energy.

these two equivalent limits, the Coulomb interaction U may be treated adiabatically. This is because in thermal equilibrium the perturbation series in U is absolutely convergent at $T = 0$ for any finite U ,²⁰⁾ and there is no phase transition at finite T . When the voltage is finite but still much larger than the other energy scales $eV \gg \max(U, |E_d|, \Delta, T)$, the behavior of $\mathbf{G}(\omega)$ at low frequencies $|\omega| \ll eV$ may be approximated reasonably by that in the $eV \rightarrow \infty$ limit.

In the case of $\Gamma_L \neq \Gamma_R$ the two limits, *i*) and *ii*), are not equivalent because the charge distribution around the impurity at $eV \rightarrow \infty$ does not correspond to that at $T \rightarrow \infty$. In this relation, we examine the $T \rightarrow \infty$ limit at finite eV . In this limit the distribution function is given by $f_{\text{eff}}(\omega)|_{T \rightarrow \infty} \equiv 1/2$ without the assumption of $\Gamma_L = \Gamma_R$, and the Green's function becomes identical to that in the $T \rightarrow \infty$ limit at $eV = 0$. Physically, this is rather obvious because at $T \gg eV$ the effects of the bias voltage are hidden by the thermal fluctuations.

3.2 Order U^2 self-energy

In order to show a rough sketch of the Green's function in the high-voltage limit, we use here the order U^2 retarded self-energy.^{11, 16, 21)} It yields a reliable picture at least qualitatively, and can be calculated analytically at $eV \rightarrow \infty$,

$$\Sigma_{\text{cor}}^{r(2)}(\omega) \Big|_{V \rightarrow \infty} = \left(\frac{U}{2} \right)^2 \frac{1}{\omega + i3\Delta}. \quad (24)$$

Here we have assumed the electron-hole symmetry taking the parameters to be $E_d = -U/2$, $\mu_L = eV/2$, $\mu_R = -eV/2$, and $\Gamma_L = \Gamma_R (= \Delta/2)$, so that the results are applicable equally to the $T \rightarrow \infty$ limit at equilibrium. Note that eq. (24) is the correlation part, which is ob-

tained by separating the Hartree-Fock contribution $U/2$ as $\Sigma^r = U/2 + \Sigma_{\text{cor}}^r$, and the retarded Green's function is given by $G^r(\omega) = [\omega + i\Delta - \Sigma_{\text{cor}}^r(\omega)]^{-1}$. Fig. 3 shows the spectral function, $\text{Im}G^r(\omega)$, obtained using the order U^2 self-energy. The Kondo resonance situated at $\omega = 0$, $eV = 0$ (dashed line) disappears at high voltages (solid line), as seen in Fig. 3(a) for $U/(\pi\Delta) = 2$. The results in the $eV \rightarrow \infty$ limit are plotted for several values of U in Fig. 3(b). For strong interactions $U \gg \Delta$ the spectral function has two peaks corresponding to the Hubbard bands at $\omega \simeq \pm U/2$, while for weak interactions $U \lesssim \Delta$ the contributions of the mixing dominate and it results in the single-peak structure. The order U^2 results could be refined quantitatively by including the higher-order terms²²⁾ or by numerical methods.

4. Low-Voltage Behavior

4.1 Ward identity

In the opposite limit, at small bias voltages $eV \ll T_K$, the low-energy properties can be described by the Fermi-liquid theory.^{15,16)} The proof has been provided in the previous paper using the Ward identity for the first and second derivatives of the self-energy with respect to eV .¹⁴⁾ We describe here the outline briefly to emphasize the properties of $\Sigma(\omega)$ as a functional of the distribution function $f_{\text{eff}}(\omega)$. Since the voltage V enters $\mathbf{G}_0(\omega)$ through $f_{\text{eff}}(\omega)$ as seen in eqs. (8)–(12), we have

$$\left. \frac{\partial}{\partial(eV)} \mathbf{G}_0(\omega) \right|_{V=0} = -\alpha \left(\frac{\partial}{\partial\omega} + \frac{\partial}{\partial E_d} \right) \mathbf{G}_{0;\text{eq}}(\omega), \quad (25)$$

$$\left. \frac{\partial^2}{\partial(eV)^2} \mathbf{G}_0(\omega) \right|_{V=0} = \kappa \left(\frac{\partial}{\partial\omega} + \frac{\partial}{\partial E_d} \right)^2 \mathbf{G}_{0;\text{eq}}(\omega). \quad (26)$$

Here $\mathbf{G}_{0;\text{eq}}(\omega) \equiv \mathbf{G}_0(\omega)|_{V=0}$ is the equilibrium Green's function, $\alpha \equiv (\alpha_L \Gamma_L - \alpha_R \Gamma_R)/(\Gamma_L + \Gamma_R)$, and $\kappa \equiv (\alpha_L^2 \Gamma_L + \alpha_R^2 \Gamma_R)/(\Gamma_L + \Gamma_R)$. The derivatives of $\Sigma(\omega)$ with respect to eV can be calculated by taking the derivative of \mathbf{G}_0 in each term of the perturbation series, and then replacing the derivative $\partial/\partial(eV)$ with $(\partial/\partial\omega + \partial/\partial E_d)$ using eqs. (25) and (26). It yields

$$\left. \frac{\partial \Sigma(\omega)}{\partial(eV)} \right|_{V=0} = -\alpha \left(\frac{\partial}{\partial\omega} + \frac{\partial}{\partial E_d} \right) \Sigma_{\text{eq}}(\omega), \quad (27)$$

$$\begin{aligned} \left. \frac{\partial^2 \Sigma(\omega)}{\partial(eV)^2} \right|_{V=0} &= \alpha^2 \left(\frac{\partial}{\partial\omega} + \frac{\partial}{\partial E_d} \right)^2 \Sigma_{\text{eq}}(\omega) \\ &+ \frac{\Gamma_L \Gamma_R}{(\Gamma_L + \Gamma_R)^2} \hat{D}^2 \Sigma_{\text{eq}}(\omega), \end{aligned} \quad (28)$$

where $\Sigma_{\text{eq}}(\omega) \equiv \Sigma(\omega)|_{V=0}$. In eq. (28), \hat{D}^2 denotes the functional operation carrying out the second derivative $(\partial/\partial\omega + \partial/\partial E_d)^2$ for all the single \mathbf{G}_0 's in the perturbation series of Σ_{eq} , which can formally be expressed using the functional differentiation of Σ_{eq} with respect to \mathbf{G}_0 ,

$$\begin{aligned} \hat{D}^2 \Sigma_{\text{eq}}(\omega) &\equiv \sum_{\nu\nu'} \int d\omega' \frac{\delta \Sigma_{\text{eq}}(\omega)}{\delta G_{0;\text{eq}}^{\nu\nu'}(\omega')} \\ &\times \left(\frac{\partial}{\partial\omega'} + \frac{\partial}{\partial E_d} \right)^2 G_{0;\text{eq}}^{\nu\nu'}(\omega'). \end{aligned} \quad (29)$$

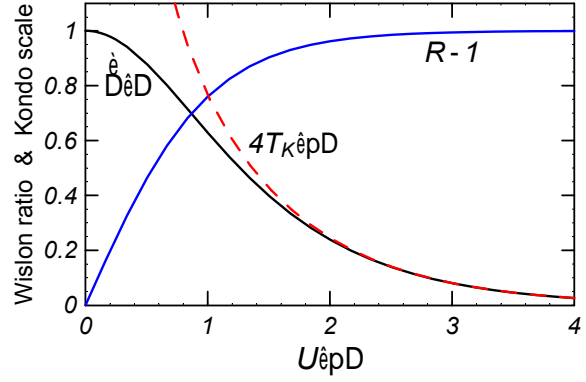


Fig. 4. The U dependence of R and $\tilde{\Delta}$: Bethe ansatz results.

Note that the perturbation series can be described in the real-frequency representation, and $\Sigma(\omega)$ can be regarded as a functional of $\mathbf{G}_0(\omega)$. Eqs. (27) and (28) relate the nonequilibrium quantities with the equilibrium ones. Especially, at $T = 0$ the usual zero-temperature formalism of the Green's function is applicable, and the right-hand side of eqs. (27) and (28) can be rewritten in terms of the vertex corrections.¹⁴⁾ Along this line, the low-energy behavior of the self-energy $\Sigma^r(\omega)$ and spectral function $A(\omega) \equiv -\text{Im}G^r(\omega)/\pi$ has been calculated exactly up to terms of order ω^2 , T^2 , and $(eV)^2$.

4.2 Experimental determination of the Wilson ratio

The low-energy behavior of the differential conductance dI/dV has also been calculated up to terms of order T^2 and $(eV)^2$ using the results of $A(\omega)$ and the formula for the nonequilibrium current eq. (C.5) given in Appendix C. Specifically, in the electron-hole symmetric case, the local Fermi liquid is characterized by two parameters, i.e., the Wilson ratio R and the energy scale $\tilde{\Delta}$ which corresponds to the width of the Kondo resonance.²³⁾ In terms of these two parameters, the low-energy behavior of $A(\omega)$ and dI/dV can be expressed in the form

$$\begin{aligned} A(\omega) &= \frac{1}{\pi\Delta} \left[1 - \left(1 + \frac{(R-1)^2}{2} \right) \left(\frac{\omega}{\tilde{\Delta}} \right)^2 \right. \\ &\quad \left. - \frac{(R-1)^2}{2} \left(\frac{\pi T}{\tilde{\Delta}} \right)^2 - \frac{3(R-1)^2}{8} \left(\frac{eV}{\tilde{\Delta}} \right)^2 + \dots \right], \end{aligned} \quad (30)$$

$$\begin{aligned} \frac{dI}{dV} &= \frac{2e^2}{h} \left[1 - \frac{1 + 2(R-1)^2}{3} \left(\frac{\pi T}{\tilde{\Delta}} \right)^2 \right. \\ &\quad \left. - \frac{1 + 5(R-1)^2}{4} \left(\frac{eV}{\tilde{\Delta}} \right)^2 + \dots \right]. \end{aligned} \quad (31)$$

These parameters contain all contributions of the perturbation series in U , and are defined with respect to the equilibrium ground state: $R \equiv \tilde{\chi}_s/\tilde{\gamma}$ and $\tilde{\Delta} \equiv \Delta/\tilde{\gamma}$ where $\tilde{\gamma}$ and $\tilde{\chi}_s$ are the enhancement factors for the T -linear specific heat and spin susceptibility, respectively.²⁴⁾ The values of these parameters can be evaluated using the

exact Bethe ansatz solution,^{20,25,26)} as shown in Fig. 4. The width of the Kondo peak $\tilde{\Delta}$ decreases monotonically with increasing U and tends to $\tilde{\Delta} \rightarrow 4T_K/\pi$ for large U , where

$$T_K = \pi\Delta\sqrt{u/(2\pi)} \exp[-\pi^2u/8 + 1/(2u)], \quad (32)$$

and $u = U/(\pi\Delta)$. The Wilson ratio increases with u from the noninteracting value $R = 1$, and converges rapidly for $u \gtrsim 2.0$ to the value of the Kondo limit $R \rightarrow 2$ reflecting the suppression of the charge fluctuations by the strong Coulomb interaction. For the quantum dots, the value of R and $\tilde{\Delta}$ can be estimated experimentally from the results of dI/dV without carrying out the measurements of the spin susceptibility and specific heat: the coefficient of the T^2 and V^2 terms of dI/dV in eq. (31) may be estimated from the observations near the unitarity limit. This is also one typical feature of the Kondo system in the quantum dots.

5. Summary

Using the functional method, the dependence of the Keldysh Green's function $\mathbf{G}(\omega)$ on eV and T has been confirmed to arise through the nonequilibrium distribution function $f_{\text{eff}}(\omega)$ which enters $\mathbf{G}_0(\omega)$. From this property, the asymptotic behavior of $\mathbf{G}(\omega)$ at high and low bias voltages has been deduced exactly. The low-voltage behavior is determined by a set parameters of the local Fermi liquid such as the Wilson ratio R and Kondo energy scale $\tilde{\Delta}$. The values of these parameters can be estimated experimentally from the T^2 and V^2 contributions of the differential conductance near the unitarity limit. In the high-voltage limit $eV \rightarrow \infty$ the Green's function becomes identical to that of the $T \rightarrow \infty$ limit at equilibrium, when the couplings between the dot and two leads are symmetric $\Gamma_L = \Gamma_R$. These results suggest that the Coulomb interaction U can be treated adiabatically at both low ($eV \ll T_K$) and high ($U \ll eV$) bias voltages.

Acknowledgements

I would like to thank A. C. Hewson, H. Ishii and S. Nonoyama for discussions. This work has been supported by the Grant-in-Aid for Scientific Research from the Ministry of Education, Science and Culture, Japan.

Appendix A: Time Evolution of Density Matrix

The time evolution of the density matrix is described by

$$\frac{\partial}{\partial t} \tilde{\rho}(t) = -i [H, \tilde{\rho}(t)]. \quad (\text{A}\cdot 1)$$

The formal solution of this equation can be obtained in the interaction representation,

$$\begin{aligned} \tilde{\rho}(t) &\equiv e^{iH_1 t} \tilde{\rho}(t_0) e^{-iH_1 t} \\ &= \mathcal{U}(t, t_0) \tilde{\rho}(t_0) \mathcal{U}(t_0, t), \end{aligned} \quad (\text{A}\cdot 2)$$

where $\mathcal{U}(t, t_0)$ is the time-evolution operator

$$\mathcal{U}(t, t_0) = \text{T exp} \left[-i \int_{t_0}^t dt' \tilde{H}_2(t') \right] \quad (\text{A}\cdot 3)$$

and $\tilde{H}_2(t) = e^{iH_1 t} H_2 e^{-iH_1 t}$. The relations among the Schrödinger \mathcal{O}_S , interaction $\tilde{\mathcal{O}}(t)$, and Heisenberg $\mathcal{O}_H(t)$ operators are

$$\tilde{\mathcal{O}}(t) = e^{iH_1 t} \mathcal{O}_S e^{-iH_1 t}, \quad (\text{A}\cdot 4)$$

$$\mathcal{O}_H(t) = \mathcal{U}(0, t) \tilde{\mathcal{O}}(t) \mathcal{U}(t, 0). \quad (\text{A}\cdot 5)$$

To describe the nonequilibrium state, the initial condition is given at $t_0 \rightarrow -\infty$ in eq. (A·2) assuming that each of the isolated leads is in the thermal equilibrium

$$\tilde{\rho}(-\infty) = \frac{e^{-\beta[H_1 - \mu_L N_L - \mu_R N_R]}}{\text{Tr} e^{-\beta[H_1 - \mu_L N_L - \mu_R N_R]}}, \quad (\text{A}\cdot 6)$$

where $N_\lambda = \sum_{k\sigma} c_{k\lambda\sigma}^\dagger c_{k\lambda\sigma}$ for $\lambda = L, R$. Then the expectation value of $\mathcal{O}_H(t)$ with respect to $\tilde{\rho}(0)$ can be written in the form of a time-ordered function along the Keldysh contour,

$$\begin{aligned} \langle \mathcal{O}_H(t) \rangle &\equiv \text{Tr} [\tilde{\rho}(0) \mathcal{O}_H(t)] \\ &= \text{Tr} \left[\tilde{\rho}(-\infty) \mathcal{U}(-\infty, +\infty) \mathcal{U}(+\infty, t) \tilde{\mathcal{O}}(t) \mathcal{U}(t, -\infty) \right]. \end{aligned} \quad (\text{A}\cdot 7)$$

Note that $\mathcal{U}(-\infty, +\infty) = \mathcal{U}^\dagger(+\infty, -\infty)$ can be expressed in terms of the anti-time-ordering operator $\tilde{\text{T}}$ as

$$\mathcal{U}(-\infty, +\infty) = \tilde{\text{T}} \exp \left[i \int_{-\infty}^{+\infty} dt' \tilde{H}_2(t') \right]. \quad (\text{A}\cdot 8)$$

Appendix B: Matrix Dyson Equation

In the matrix notation used in eq. (13), the Dyson equation for the intra-site Green's function at the dot $\mathbf{G}(\omega)$ and that for the inter-site ones between the dot and leads are given by

$$\begin{aligned} \mathbf{G}(\omega) &= \mathbf{g}(\omega) + \mathbf{g}(\omega) \boldsymbol{\Sigma}(\omega) \mathbf{G}(\omega) \\ &\quad + v_L \mathbf{g}(\omega) \boldsymbol{\tau}_3 \mathbf{G}_{Ld}(\omega) + v_R \mathbf{g}(\omega) \boldsymbol{\tau}_3 \mathbf{G}_{Rd}(\omega), \end{aligned} \quad (\text{B}\cdot 1)$$

$$\mathbf{G}_{\lambda d}(\omega) = v_\lambda \mathbf{g}_\lambda(\omega) \boldsymbol{\tau}_3 \mathbf{G}(\omega), \quad (\text{B}\cdot 2)$$

$$\mathbf{G}_{d\lambda}(\omega) = v_\lambda \mathbf{G}(\omega) \boldsymbol{\tau}_3 \mathbf{g}_\lambda(\omega), \quad (\text{B}\cdot 3)$$

$$\boldsymbol{\tau}_3 = \begin{bmatrix} 1 & 0 \\ 0 & -1 \end{bmatrix}, \quad \mathbf{P} = \frac{1}{\sqrt{2}} \begin{bmatrix} 1 & 1 \\ -1 & 1 \end{bmatrix}. \quad (\text{B}\cdot 4)$$

Here the elements of $\mathbf{G}_{\lambda d}(t)$ and $\mathbf{G}_{d\lambda}(t)$ are defined by $G_{\lambda d}^{--}(t) = -i \langle \text{T} c_{\lambda\sigma}(t) d_\sigma^\dagger(0) \rangle$, \dots , and $G_{d\lambda}^{--}(t) = -i \langle \text{T} d_\sigma(t) c_{\lambda\sigma}^\dagger(0) \rangle$, \dots , respectively. The Green's functions for the isolated leads $\mathbf{g}_\lambda(\omega)$ include the distribution functions for the initial state,

$$\mathbf{g}_\lambda(\omega) = \mathbf{P} \begin{bmatrix} 0 & g_\lambda^a(\omega) \\ g_\lambda^r(\omega) & g_\lambda^k(\omega) \end{bmatrix} \mathbf{P}^{-1}, \quad (\text{B}\cdot 5)$$

$$g_\lambda^r(\omega) = \sum_k \frac{|\phi_{k\lambda}(r_\lambda)|^2}{\omega - \epsilon_{k\lambda} + i0^+}, \quad (\text{B}\cdot 6)$$

$$g_\lambda^K(\omega) \equiv [1 - 2f_\lambda(\omega)][g_\lambda^r(\omega) - g_\lambda^a(\omega)]. \quad (\text{B}\cdot 7)$$

For the isolated dot, the Green's function can be written as $\{\mathbf{g}(\omega)\}^{-1} = (\omega - E_d)\boldsymbol{\tau}_3$. Note that the contribution of the element $g^K(\omega)$ which corresponds to eq. (B·7) vanishes for the isolated dot because of a property $\{g^r(\omega)\}^{-1}g^K(\omega)\{g^a(\omega)\}^{-1} = 0$.¹¹⁾ Using eqs. (B·1) and (B·2), we have

$$\{\mathbf{G}(\omega)\}^{-1} = \{\mathbf{G}_0(\omega)\}^{-1} - \boldsymbol{\Sigma}(\omega), \quad (\text{B}\cdot 8)$$

$$\{\mathbf{G}_0(\omega)\}^{-1} \equiv \{\mathbf{g}(\omega)\}^{-1} - \boldsymbol{\sigma}(\omega), \quad (\text{B}\cdot 9)$$

$$\boldsymbol{\sigma}(\omega) \equiv v_L^2 \boldsymbol{\tau}_3 \mathbf{g}_L(\omega) \boldsymbol{\tau}_3 + v_R^2 \boldsymbol{\tau}_3 \mathbf{g}_R(\omega) \boldsymbol{\tau}_3. \quad (\text{B}\cdot 10)$$

Then, using eqs. (B·5)–(B·7), $\boldsymbol{\sigma}(\omega)$ is written in the form

$$\boldsymbol{\sigma}(\omega) = \mathbf{P} \begin{bmatrix} \Omega_0(\omega) & \sigma^r(\omega) \\ \sigma^a(\omega) & 0 \end{bmatrix} \mathbf{P}^{-1}, \quad (\text{B}\cdot 11)$$

$$\sigma^r(\omega) = v_L^2 g_L^r(\omega) + v_R^2 g_R^r(\omega), \quad (\text{B}\cdot 12)$$

$$\Omega_0(\omega) = v_L^2 g_L^K(\omega) + v_R^2 g_R^K(\omega). \quad (\text{B}\cdot 13)$$

When the density of states $\text{Im } g_\lambda^r(\omega)$ is a constant and its band width is infinity, $\sigma^r(\omega)$ becomes pure imaginary as $v_\lambda^2 g_\lambda^r(\omega) = -i\Gamma_\lambda$. We obtain the explicit form of $\mathbf{G}_0(\omega)$ given by eqs. (8)–(11) via eq. (B·9). Through eq. (B·8), $\mathbf{G}(\omega)$ can be expressed in similar forms;

$$G^{--}(\omega) = [1 - \tilde{f}_{\text{eff}}(\omega)]G^r(\omega) + \tilde{f}_{\text{eff}}(\omega)G^a(\omega), \quad (\text{B}\cdot 14)$$

$$G^{++}(\omega) = -\tilde{f}_{\text{eff}}(\omega)[G^r(\omega) - G^a(\omega)], \quad (\text{B}\cdot 15)$$

$$G^{+-}(\omega) = [1 - \tilde{f}_{\text{eff}}(\omega)][G^r(\omega) - G^a(\omega)], \quad (\text{B}\cdot 16)$$

$$G^{++}(\omega) = -[1 - \tilde{f}_{\text{eff}}(\omega)]G^a(\omega) - \tilde{f}_{\text{eff}}(\omega)G^r(\omega), \quad (\text{B}\cdot 17)$$

where $G^r(\omega)$ and $\tilde{f}_{\text{eff}}(\omega)$ are given by

$$G^r(\omega) = \frac{1}{\omega - E_d - \sigma^r(\omega) - \Sigma^r(\omega)}, \quad (\text{B}\cdot 18)$$

$$\tilde{f}_{\text{eff}}(\omega) \equiv \frac{f_L(\omega)\Gamma_L + f_R(\omega)\Gamma_R - \frac{1}{2i}\Sigma^{-+}(\omega)}{\Gamma_L + \Gamma_R - \text{Im}\Sigma^r(\omega)}. \quad (\text{B}\cdot 19)$$

Here $\tilde{f}_{\text{eff}}(\omega)$ is real because $\Sigma^{-+}(\omega)$ is pure imaginary, and at equilibrium it becomes the usual Fermi function since $\Sigma^{-+}(\omega)|_{V=0} = 2i f(\omega) \text{Im } \Sigma^r(\omega)|_{V=0}$.¹¹⁾ Note that $\Sigma^r = \Sigma^{--} + \Sigma^{-+}$. There are some additional relations: $\Sigma^a(\omega) = \{\Sigma^r(\omega)\}^*$, and $\Sigma^{--}(\omega) = -\{\Sigma^{++}(\omega)\}^*$.

Appendix C: Current and Charge

The operator for the current flowing from the left lead to the dot I_L and that from the dot to the right lead I_R are given by

$$I_\lambda = ie w_\lambda \sum_\sigma v_\lambda \left(c_{\lambda\sigma}^\dagger d_\sigma - d_\sigma^\dagger c_{\lambda\sigma} \right), \quad (\text{C}\cdot 1)$$

where $w_R = 1$ and $w_L = -1$. The equation of continuity is written as $\partial n_d / \partial t + I_R - I_L = 0$ with $n_d = \sum_\sigma n_{d\sigma}$.

The averages of these operators with respect to $\hat{\rho}(0)$ are

$$\langle n_d \rangle = 2 \int_{-\infty}^{\infty} \frac{d\omega}{2\pi i} G^{-+}(\omega), \quad (\text{C}\cdot 2)$$

$$\langle I_\lambda \rangle = 2e w_\lambda \int_{-\infty}^{\infty} \frac{d\omega}{2\pi} v_\lambda [G_{d\lambda}^{-+}(\omega) - G_{\lambda d}^{-+}(\omega)]. \quad (\text{C}\cdot 3)$$

Note that $G_{\lambda d}^{-+}$ and $G_{d\lambda}^{-+}$ can be expressed in terms of \mathbf{G} using eqs. (B·2)–(B·3). Specifically, if the couplings with the leads satisfy a condition $\Gamma_L(\omega) \propto \Gamma_R(\omega)$, the expectation value of the current can be rewritten as²⁷⁾

$$I = \frac{\Gamma_L \langle I_R \rangle + \Gamma_R \langle I_L \rangle}{\Gamma_R + \Gamma_L} \quad (\text{C}\cdot 4)$$

$$= \frac{2e}{h} \int_{-\infty}^{\infty} d\omega [f_L - f_R] \frac{4\Gamma_L \Gamma_R}{\Gamma_R + \Gamma_L} [-\text{Im } G^r(\omega)]. \quad (\text{C}\cdot 5)$$

Note that $\langle I_L \rangle = \langle I_R \rangle$ in the stationary state.

- 1) D. Goldharber-Gordon, *et al.*: Nature **391** (1998) 156.
- 2) S. M. Cronenwett *et al.*: Science **281** (1998) 540.
- 3) F. Simmel *et al.*: Phys. Rev. Lett. **83** (1999) 804.
- 4) W. G. van der Wiel, *et al.*: Science **289** (2000) 2105.
- 5) T. K. Ng and P. A. Lee: Phys. Rev. Lett. **61** (1988) 1768.
- 6) L. I. Glazman and M. E. Raikh: JETP Lett. **47** (1988) 452.
- 7) A. Kawabata: J. Phys. Soc. Jpn. **60** (1991) 3222.
- 8) A. C. Hewson: *The Kondo Problem to Heavy Fermions* (Cambridge University Press, Cambridge, 1993).
- 9) W. Izumida, O. Sakai, and S. Suzuki: J. Phys. Soc. Jpn. **70** (2001) 1045.
- 10) N. S. Wingreen and Y. Meir: Phys. Rev. B **49** (1994) 11040.
- 11) S. Hershfield, J. H. Davies, and J. W. Wilkins: Phys. Rev. B **46** (1992) 7046.
- 12) A. Yeyati *et al.*: Phys. Rev. Lett. **71** (1993) 2991; M. H. Hettler *et al.*: Phys. Rev. Lett. **73** (1994) 1967; A. Schiller and S. Hershfield: Phys. Rev. B **58** (1998) 14978; H. Schoeller and J. König: Phys. Rev. Lett. **84** (2000) 3686; P. Coleman *et al.*: cond-mat/0108001; Phys. Rev. Lett. **86** (2001) 4088; A. Rosch, *et al.*: Phys. Rev. Lett. **87** (2001) 156802.
- 13) A. Kaminski, Yu. V. Nazarov, and L. I. Glazman: Phys. Rev. B **62** (2000) 8154.
- 14) A. Oguri: Phys. Rev. B **64** (2001) 153305.
- 15) P. Nozières: J. Low Temp. Phys. **17** (1974) 31.
- 16) K. Yamada: Prog. Theor. Phys. **53** (1975) 970; Prog. Theor. Phys. **54** (1975) 316.
- 17) J. M. Luttinger and J. C. Ward: Phys. Rev. **118** (1960) 1417.
- 18) L. V. Keldysh: Sov. Phys. JETP **20** (1965) 1017; C. Caroli, *et al.*: J. Phys. C **4** (1971) 916. We have used the notation given by E. M. Lifshitz and L. P. Pitaevskii, *Physical Kinetics* (Pergamon Press, Oxford, 1981).
- 19) See, for instance, K. C. Chou *et al.*: Phys. Rep. **118** (1985) 1; J. W. Negele and H. Orland: *Quantum Many-Particle Systems* (Addison-Wesley, Redwood City, 1987).
- 20) V. Zlatić and B. Horvatić: Phys. Rev. B **28** (1983) 6904.
- 21) B. Horvatić, D. Šokčević, and V. Zlatić: Phys. Rev. B **36** (1987) 365.
- 22) D. E. Logan and N. L. Dickens: J. Phys.: Condes. Matter **14** (2002) 3605.
- 23) A. C. Hewson: Adv. Phys. **43** (1994) 543.
- 24) $\tilde{\gamma} \equiv 1 - \partial \Sigma^r(\omega) / \partial \omega|_{\omega=0}$ and $\tilde{\chi}_s = \tilde{\chi}_{\uparrow\uparrow} - \tilde{\chi}_{\uparrow\downarrow}$ with $\tilde{\chi}_{\sigma\sigma'} \equiv \delta_{\sigma\sigma'} - \partial \Sigma_\sigma^r(0) / \partial h_{\sigma'}|_{h_{\sigma'}=0}$, where $h_{\sigma'}$ is an external field described by $H_{\text{ex}} = -\Sigma_\sigma h_\sigma n_{d\sigma}$. Note that $\tilde{\gamma} = \tilde{\chi}_{\uparrow\uparrow}$.¹⁶⁾
- 25) N. Kawakami and A. Okiji: Solid State Commun. **43** (1982) 467.
- 26) B. Wiegman and A. M. Tselick: J. Phys. C **16** (1983) 2281.
- 27) Y. Meir and N. S. Wingreen: Phys. Rev. Lett. **68** (1992) 2512.